4

Quasi-planar Chiral Materials for Microwave Frequencies

Ismael Barba[1], A.C.L. Cabeceira[1], A.J. García-Collado[2], G.J. Molina-Cuberos[2], J. Margineda[2] and J. Represa[1]
[1]*University of Valladolid*
[2]*University of Murcia*
Spain

1. Introduction

The growing development in the new communication technologies requests devices to perform new features or to improve the old ones. The trend is to develop new artificial materials reproducing well-known properties already present in other frequency ranges (such as optics) or materials with properties inexistent in the nature. Among the first kind, artificial chiral media, based on the random inclusion of metallic particles with chiral symmetry into a host medium are worth to mention (Fig. 1). Nevertheless, the fabrication techniques up-to-date are quite expensive and produce samples not easy to be tailored and with imperfections, such as intrinsic anisotropy and non-homogeneity (non-uniform density and orientation of inclusions), as well as heavy losses.

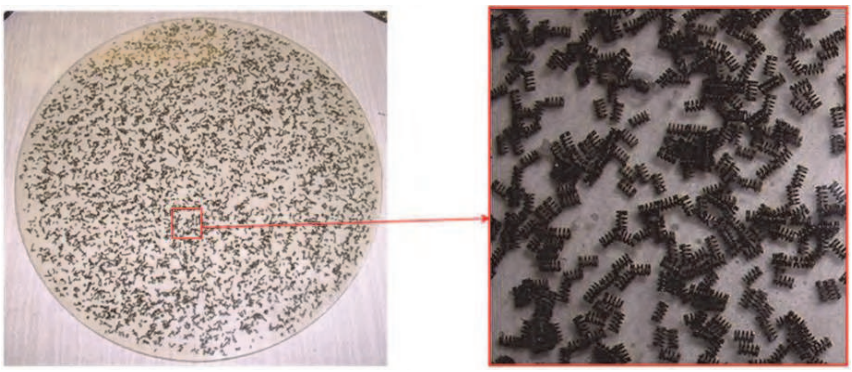

Fig. 1. Helix-based artificial chiral material. The sample is a 30 cm diameter disk fabricated by dispersion of six-turn stainless-steel helices in an epoxy resin with a low curing temperature. The helices are 2 mm height and 1.2 mm outer diameter.

During the last years, alternative methods, based on a periodic distribution of planar or quasi-planar chiral particles, have been proposed. This alternative presents the possibility of using conventional printed-circuit fabrication techniques to manufacture the structure. At the same time, the use of via holes provides additional flexibility to select the type of

inclusions from helices to cranks or even pseudo-chiral inclusions such as Ω's. As a consequence, the realization of the bulk material, staggering printed circuit plates, gives rise to axial anisotropy.

In this chapter, we are going to present some of the research performed during the last years in the field of chiral materials implementation by means of quasi-planar technologies. Section 2 presents an introduction on chiral materials, as well as (2.2) different approaches in order to implement them: traditional (random) distribution and new, periodic distributions. In the last case, we present different alternative (planar) implementations, finishing with our own (quasi-planar) proposal.

Section 3 shows the two complementary analysis techniques we have employed: numerical analysis, as well as experimental measures, both in free and guided propagation, with a previous fabrication of the samples. Finally, we present (section 4) the results we have obtained (rotation angle of polarization).

2. Chiral materials

Chiral materials are characterized by asymmetric microstructures in such a way that those structures and their mirror images are not superimposable. As a consequence, right- and left-hand circularly polarized waves propagate through the material with different phase velocities and, in case the medium is lossy, absorption rates. Electromagnetic waves in chiral media show the following interesting behavior (Lindell et al., 1994):

1. Optical (electromagnetic) rotatory dispersion (ORD), causing a rotation of polarization;
2. Circular dichroism (CD): due to the different absorption coefficients of a right- and left-handed circularly polarized wave, the nature of field polarization is modified, making linear polarization of a wave to change into elliptical polarization.

These properties have drawn considerable attention to chiral media and may open new potential applications in microwave and millimeter-wave technology: antennas and arrays (Lakhtakia et al., 1988; Viitanen et al., 1998), twist polarizers (Lindell et al., 1992), antireflection coatings (Varadan et al., 1987; Kopyt 2010), etc. It has been also proposed as a way to achieve negative refraction index (Pendry, 2004; Tretyakov et al., 2005). Also, many papers on the analysis of free and guided electromagnetic wave propagation through chiral media have been published, both in time (González-García et al., 1998; Demir et al., 2005; Pereda et al., 2006) and frequency (Xu et al., 1995; Alú et al., 2003; Pitarch et al., 2007; Gómez et al., 2010) domain. For this reason, during the last years, there has been an extensive research on new designs that enhance the above-mentioned properties, as we will see in the next sections of this chapter.

2.1 Constitutive relationships

In contrast to isotropic materials, characterized by their permittivity and permeability, bi-isotropic materials show a cross coupling between electric and magnetic fields, their constitutive relations being:

$$\begin{aligned} \vec{D} &= \varepsilon \vec{E} + \eta \vec{H} \\ \vec{B} &= \zeta \vec{E} + \mu \vec{H} \end{aligned} \tag{1}$$

where the four scalars ε, μ, η, ζ are function of frequency ω. When the following condition holds:

$$\zeta = -\eta = \frac{j\kappa}{c_0} \tag{2}$$

c_0 being light speed in vacuum, the medium is said to be "chiral". The parameter κ is the "chirality" or "Pasteur" parameter (Lindell et al., 1994). In the frequency domain, this leads to the following constitutive relationships:

$$\begin{aligned} \vec{D}(\omega) &= \varepsilon \vec{E}(\omega) - \frac{j\kappa(\omega)}{c_0}\vec{H}(\omega) \\ \vec{B}(\omega) &= \mu \vec{H}(\omega) + \frac{j\kappa(\omega)}{c_0}\vec{E}(\omega) \end{aligned} \tag{3}$$

The real part of the chirality parameter is related with the rotation angle of the polarization plane (ORD) in a distance d by means of the following expression:

$$\theta = 2d\omega\frac{\kappa'}{c_0} \tag{4}$$

Considering electromagnetic field propagation through a homogeneous chiral medium, it is convenient to introduce new field variables, $\vec{E}_{\pm}$ and $\vec{H}_{\pm}$ ("wavefield vectors"), being the following linear combinations of the electric and magnetic fields:

$$\vec{E}_{\pm} = \frac{1}{2}\left(\vec{E} \mp jZ\vec{H}\right), \vec{H}_{\pm} = \frac{1}{2}\left(\vec{H} \pm \frac{j}{Z}\vec{E}\right) \tag{5}$$

where Z is the wave impedance of the medium, $Z = \sqrt{\mu/\varepsilon}$. Actually, the two wavefields $\{\vec{E}_+, \vec{H}_+\}$ and $\{\vec{E}_-, \vec{H}_-\}$ are plane right-circularly and left-circularly polarized waves, respectively. The advantage of introducing these new vectors is that they satisfy the Maxwell equations in an equivalent isotropic medium, so we may use well-known solutions for fields in simple isotropic medium to obtain solutions for wave propagation through chiral media (Lindell et al., 1994). These wavefield vectors will "see" equivalent simple isotropic media with the equivalent parameters:

$$\varepsilon_{\pm} = \varepsilon\left(1 \pm \frac{\kappa}{\sqrt{\varepsilon\mu}}\right), \ \mu_{\pm} = \mu\left(1 \pm \frac{\kappa}{\sqrt{\varepsilon\mu}}\right) \tag{6}$$

It is clear that, if κ is high enough, one of the wavefield vectors correspond to a backward wave (Tretyakov et al., 2005). That means that, for one of the two possible circularly polarized waves, travelling through a highly chiral material, this one behaves as a left-handed (Veselago) metamaterial.

2.2 Chiral implementations

2.2.1 Random distributions

Traditionally, artificial chiral media at microwave frequencies are fabricated by embedding conducting helices into a host, as shown in Fig 1. The dimensions of these helices determine the bandwidth where the optical activity takes place (Lindman, 1920; Tretyakov et al., 2005). Nevertheless, chirality is a geometrical aspect, therefore helices are not the only possibility,

so other type of inclusions, like metal cranks (Molina-Cuberos et al., 2009; Cloete et al., 2001) have been proposed also; an example may be seen in Fig. 2.

Fig. 2. Crank-based artificial chiral material. Chiral elements were produced from a 0.4 mm diameter and 12.6 mm length copper wire by bending in three segments by two 90 angles, all with the same handedness. The elements were dispersed in an epoxy resin with a low curing temperature (Molina-Cuberos et al., 2009).

In any case, it is necessary to be careful with the fabrication procedure to assure isotropy and homogeneity. The inclusions must be randomly oriented with no special direction. If the particles are placed in an aligned configuration, the result is a macroscopically bianisotropic material, leading to matrix coefficients for the constitutive parameters (Lindell et al., 1994). Also, a random distribution trends to present local density variations and accidental alignments (see detail in Fig. 1), which causes spatial variations of the constitutive relationships. At the same time, this procedure involves other drawbacks like high cost and difficulty in cutting and molding the material.

In the case of random distribution of cranks, the problems associated to the lack of homogeneity are enhanced. For the same total wire length cranks are bigger than helices, which makes the number density of cranks to be lower than the one using helices and increases the inhomogeneity. Molina-Cuberos et al. (2009) found fluctuations of the transmitted wave depending on the sample position and orientation with respect to the antenna. Therefore, several measurements and a mean value of the rotation angle were carried out.

2.2.2 Periodical distributions

The problems associated to the lack of homogeneity in chiral media based on random distribution of particles as helices or cranks can be reduced or even eliminated by designing periodical lattices. By an adequate distribution of metallic cranks is possible to build chiral media with homogeneous, isotropic and reciprocal behavior at microwave range (García-Collado et al., 2010), Fig. 3 shows an example of such medium.

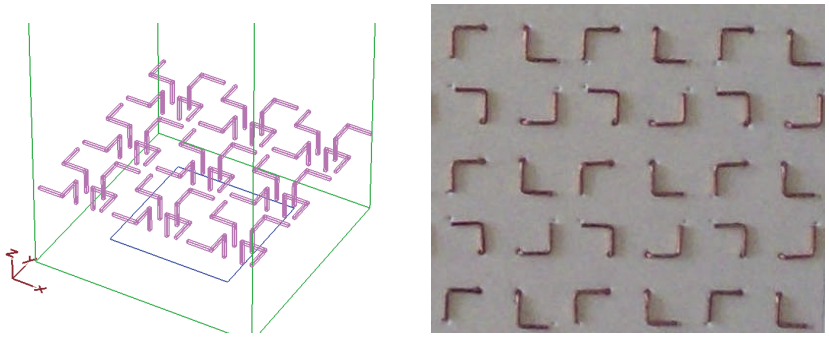

Fig. 3. Detailed view of a periodical lattice of cranks with the same handedness produced from 0.68 mm diameter and 15 mm length copper wire by bending in three segments by two 90 degrees angles. One of the segments is introduced perpendicularly into the host medium, polyurethane foam with a relative permittivity close to one. The backside of the medium is completely free of metal. Right: photograph of the lattice (García-Collado et al., 2010). Left: MEFIsTo™ model in which we may see the geometry of the cranks

For these reasons, alternative methods of manufacturing chiral materials have been proposed in recent years: Pendry et al. (Pendry et al.; 2004) proposed a periodical distribution of twisted Swiss-rolls, Kopyt et al. (Kopyt et al.; 2010) a distribution of chiral honeycombs. Nevertheless, most of the alternatives rely on planar and quasi-planar technologies, like Printed Circuit Board (PCB) technology, or even integrated circuit technology, for THz and optical materials. They provide a low-cost technique, which allows a high flexibility in the design of the elementary cell.

Planar technologies make use of two-dimensional elements, in order to obtain media with chiral response. The general concept of chirality, from a geometrical point of view, can be defined in a plane geometry (two dimensions): a structure is considered to be chiral in a plane if it cannot be brought into congruence with its mirror image, unless it is lifted from the plane (Le Guennec, 2000a, 2000b). In this case, it is possible to design a 2D-chiral medium consisting on flat elements possessing no line of symmetry in the plane, and which allows the use of planar technology to manufacture it.

However, electromagnetic activity (electromagnetic rotatory dispersion and circular dichroism) is a phenomenon that takes place in the three dimensional space. Some authors have tried to find electromagnetic activity in thus 2D structures: Papakostas et al. (2003) found a rotation of the polarization plane of a wave incident on a 2D-chiral planar structure like showed in Fig. 4, remarking its apparently nonreciprocal nature: when observed from the back side instead of the front, the sense of the twist is reversed, suggesting then a nonreciprocal polarization rotation similar to that observed in the Faraday effect. That interpretation of this result has opened a discussion on the possibility of a violation of reciprocity and time reversal symmetry (Schwanecke et al., 2003). Kuwata-Gonokami et al.

(2005) concluded that such structures are actually chiral in 3D (taking into account air-metal and substrate-metal interfaces), and their electromagnetic activity must arise from this three dimensional nature.

Fig. 4. Planar chiral structure made by arrays of gammadions arranged in two-dimensional square gratins (Papakostas et al., 2003).

Other groups have achieved three-dimensional chirality by means of multilayered structures of plane elements. The elements may be 2D-chiral (Rogacheva et al., 2006; Plum et al., 2007, 2009) or even non chiral (Zhou et al., 2009): in both cases, the 3D-chirality is obtained by means of a twist between layers (Fig. 5). These structures resulted to give an extremely strong rotation, as well as a negative index of refraction for one of the circularly polarized waves.

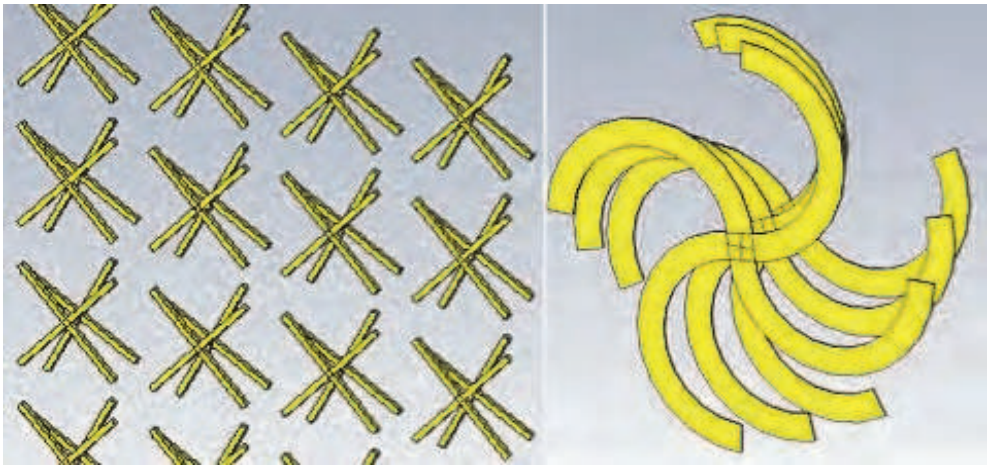

Fig. 5. Left: schematic representation of a chiral "cross-wire" simple like the one studied by Zhou et al. (2009). Right: schematic representation of a unit cell of a chiral structure, constructed from planar metal rosettes separated by a dielectric slab (Rogacheva et al., 2006; Plum et al., 2007, 2009)

Finally, it is possible also to construct 3D chiral samples using of quasi-planar technology: in this case, three dimensional PCB technology is employed, involving two-sided boards plus the use of via holes to connect both sides of the board. Such approximation was proposed by Marqués et al. (2007) and also by the authors of this chapter (Molina-Cuberos et al., 2009; Barba et al., 2009).

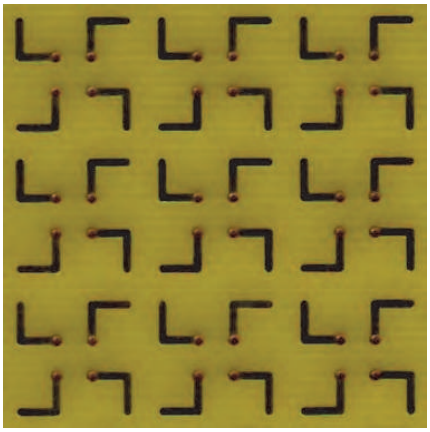

Fig. 6. Photograph of a structure similar to the shown in Fig. 3, but manufactured by means of Printed Circuit technology.

In our research, we have designed different chiral distributions of "molecules" and implemented them by different means: one (Fig. 3) is made by using metal cranks introduced into a polyurethane tablet; the second one (Fig. 6) is, as mentioned, made using PCB technology. We have designed and analyzed different distributions; some of them have been implemented and their behavior measured experimentally, while other ones have been modeled using numerical techniques. More details may be read in the following sections.

3. Analysis

We have worked, first, with the numerical analysis of the designed materials, which allows the study of their electromagnetic behavior at high frequency, previous to the effective construction of the same ones. We have used two different commercially available software in time domain:

a. MEFiSTo™, based on TLM method.
b. CST Studio Suite™ 2009, based on the finite integration technique (FIT).

Both methods are complete tools to solve electromagnetic problems in 3D, allowing the graphic visualization of the electromagnetic field propagation and its interaction with materials and boundaries during the simulation. The principal advantage of simulating in the time domain is that it most closely resembles the real world. In our case, it allows to obtain a very broadband data with a single simulation run with much less memory requirements than required in frequency-domain methods.

The experimental set-up used is based on a previous one for permittivity and permeability measurements at X-band (8.2 - 12.4 GHz) (Muñoz et al., 1998), and adapted to measure electromagnetic activity (Molina-Cuberos et al., 2009; García-Collado et al., 2010). Fig. 7

shows a diagram of the experimental set-up, where the incident wave is linearly polarized in the vertical direction.

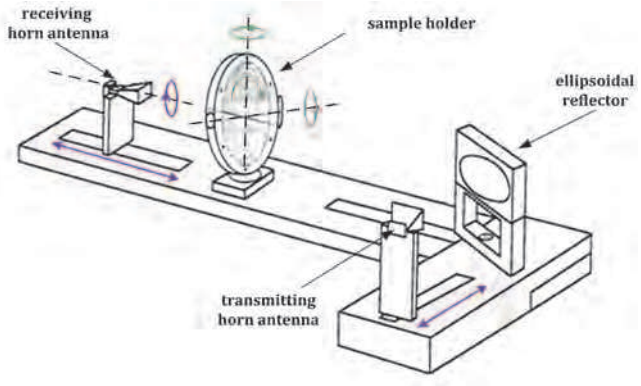

Fig. 7. Schematic diagram of the free space setup for the experimental determination of the rotation angle and the three constitutive parameters of isotropic chiral material in the X-Band (not to scale).

The transmitting and receiving antennas are 10-dB-gain rectangular horns. An incident beam is focused by an ellipsoidal concave mirror (30 cm x 26 cm), which produces a roughly circular focal area of about 6 cm in diameter, which is lower than sample size, so that diffraction problems are avoided with relatively small samples. The transmitting antenna is placed at one of the mirror foci (35 cm) and the sample at the other one. The sample holder is midway between the mirror and the receiving antenna and is able to rotate around the two axes perpendicular to the direction of propagation. The receiving antenna, located at 35 cm from the sample, can rotate about the longitudinal axis, which allows the measurement of the scattering parameters (S parameters) corresponding to any polar transmission. The interested reader is referred to Muñoz et al. (1998), Gómez et al. (2008) and García-Collado et al., (2010) for a detailed description of the measurement setup and technique. Here, we briefly present the measurement process:

Fig. 8. Waveguide setup for the experimental determination of the rotation angle produced by a chiral material in X-band. A cylindrical sample is located in the circular waveguide and fed through port 1. The transmitted wave is measured in port 2 by a rotating connection, which allows determining the component of the electrical field parallel to the TE_{10} mode of the rectangular wave.

First a two-port "through-reflect-line"' (TRL) calibration is performed at the two waveguide terminals of the network analyzer, PNA-L N5230A, where the antennas are connected. Then, a time domain (TD) transform is used to filter out mismatches from the antennas, edge diffraction effects, and unwanted multiple antenna-mirror-sample reflections or reflections from other parts of the system by means of the ``gating'' TD option of the network analyzer. The rotation angle of the transmitted polarization ellipse is defined as the difference between the polarization direction of the incident wave and the direction of the major axis of the transmitted elliptically polarized wave. Rotation can be determined by looking for the minimum value of the transmitted wave or by measuring the transmission coefficient for co- and cross-polarization, S_{21CO} and S_{21CR} (Balanis, 1989):

$$\begin{aligned} OA &= \left[\frac{1}{2}\left(S_{21CO}^2 + S_{21CR}^2 + \left(S_{21CO}^4 + S_{21CR}^4 + 2S_{21CO}^2 S_{21CR}^2 \cos(2\phi)\right)^{1/2}\right)\right]^{1/2} \\ OB &= \left[\frac{1}{2}\left(S_{21CO}^2 + S_{21CR}^2 - \left(S_{21CO}^4 + S_{21CR}^4 + 2S_{21CO}^2 S_{21CR}^2 \cos(2\phi)\right)^{1/2}\right)\right]^{1/2} \\ \tau &= \frac{\pi}{2} - \frac{1}{2}\tan^{-1}\left(\frac{2S_{21CO}S_{21CR}}{S_{21CO} - S_{21CR}}\cos(2\phi)\right) \end{aligned} \tag{7}$$

where OA and OB are the major and minor axes, respectively, ϕ the phase difference between S_{21CO} and S_{21CR}, and τ the tilt of the ellipse, relative to the incident wave.
In principle, the precise angle of rotation cannot be determined by this measurement alone, there is an uncertainty of $2n\pi$, where n is an integer. To determine the angle uniquely, we make use of measurements far away from the resonance range, where it is expected, and found that the rotation angle goes to zero. Once the scattering coefficients are known, it is also possible to retrieve the constitutive parameters (ε, μ, κ) of the sample.

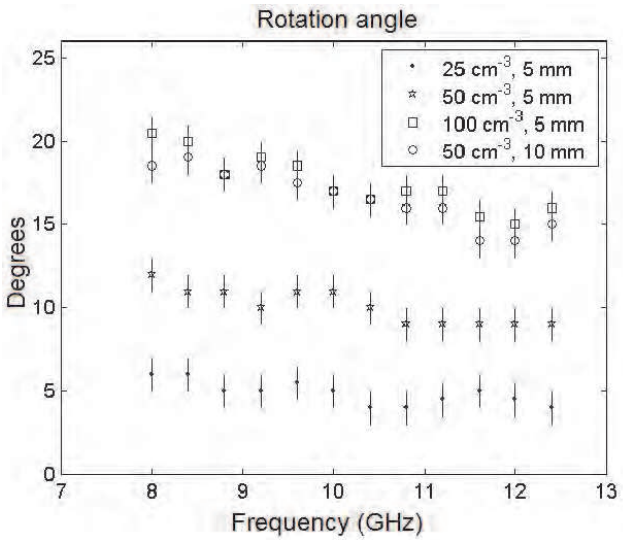

Fig. 9. Rotation angle produced by a random distribution of helices (Fig. 1) in a host, for different helix densities (25 cm^{-3}, 50 cm^{-3}, 100 cm^{-3}) and sample thickness (5 mm, 10 mm).

Several analyses of the chiral effects, by making use of waveguide setup, have been also developed; see for example Brewitt-Taylor et al. (1999). In order to test the effect of metallic cranks in waveguide, some samples were initially designed to produce chiral isotropic materials with a resonance frequency at X-band and placed into a section of circular waveguide. Fig. 8 shows the experimental set-up. The sample is excited in a rectangular waveguide and fed to the circular waveguide through a rectangular-circular waveguide transition, the dominant mode in the rectangular waveguide is TE_{10}, and the polarization is perpendicular to the resistive film of the transition which absorbs any cross-polarized field. The dominant mode is TE_{11}, in the empty circular waveguide, and $HE\pm_{11}$ in the chirowaveguide. After the sample, a section of circular waveguide, which can rotate around the longitudinal axis, is connected to a rectangular guide through a transition. The rotation angle of the transmitted wave is obtained by measuring the minimum value of the transmitted wave; we have found that this procedure is more accurate than the determination of the maximum on the transmitted wave.

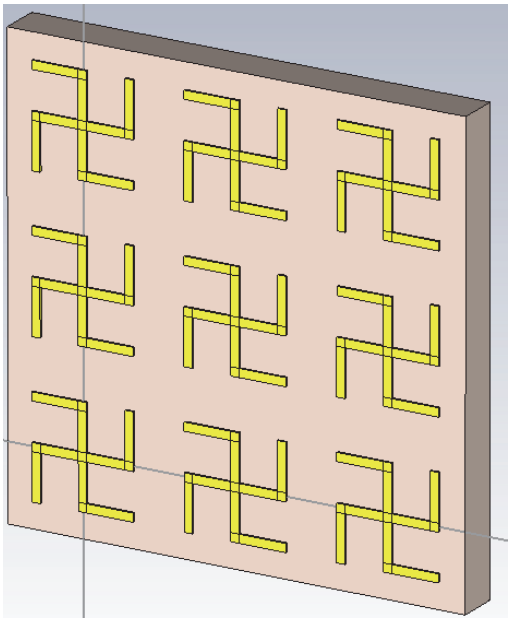

Fig. 10. Schematic illustration of an array of gammadions, chiral in 2D. Each gammadion is assumed to be of copper, and occupies a square of 6x6 mm. There is a separation of 3 mm between each gammadion. The board is 2.5 mm thick.

4. Results

4.1 Random distributions (helices)

Fig. 9 shows the rotation angle produced by a distribution of helices in a host medium for densities ranging from 0 cm^{-3} to 100 cm^{-3}, the error bars showing the uncertainties in the angle determination. Chiral elements are six-turn stainless-steel helices that are 2 mm long and 1.2 mm in outer diameter. The elements were dispersed in an epoxy resin with a low

curing temperature. We observe that the rotation angle decreases when the frequency increases, which means that the resonance frequency is below the measurement range. As it can be expected, the rotation angle increases with the number density of inclusions and with the sample width, following a nearly linear relation. Similar behavior has been found in other experiments with helices (Brewitt-Taylor et al., 1999) or cranks (Molina-Cuberos et al., 2005).

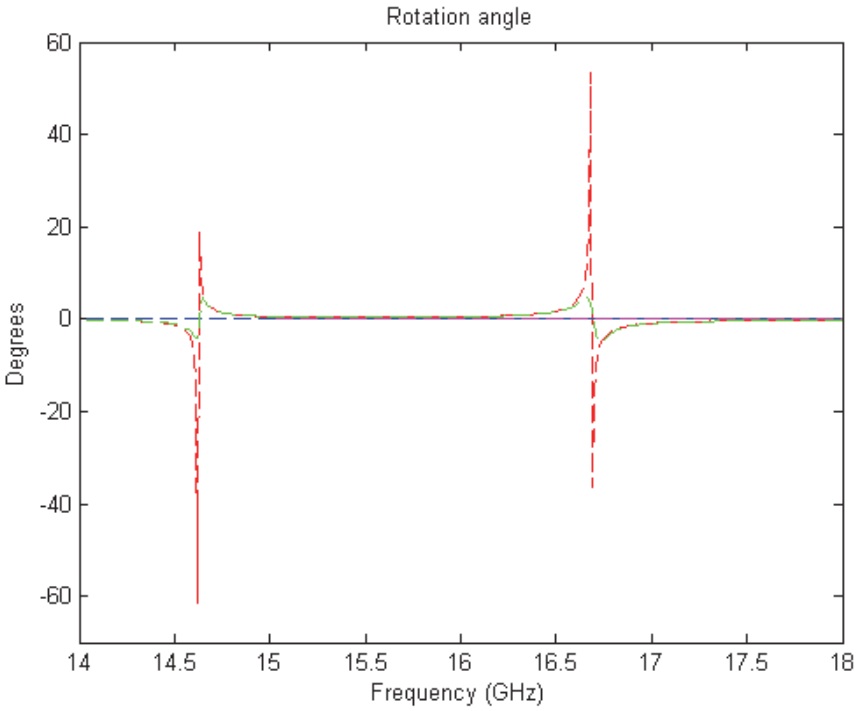

Fig. 11. Rotation of the polarization plane for a plane wave normally incident over a planar array of gammadions (Fig. 10), and for different supporting boards: free space (magenta), FR4 (blue), unlossy CER-10 (green) and lossy CER-10 (red). The result is the same in front and back incidence.

4.2 Planar distributions

We have modeled, using CST Studio Suite™ 2009, the rotation of the polarization plane, for a plane wave normally incident over a plane structure, similar, at a different scale, to the one studied by Papakostas et al. (2003). Our structure is also an array of gammadions (Fig. 10) that, in this case, presents resonance in the microwave band. The rotation has been determined assuming different properties of the board that supports the array: first assuming it has the same properties as vacuum, second, a typical material on PC Boards (FR4, $\varepsilon_r \approx 4.3$) and, finally, a high permittivity material, like Taconic CER-10 ($\varepsilon_r \approx 10$), all present in CST Studio Suite™ 2009 library. The results are shown in Fig. 11. In the first case (vacuum), the structure is symmetrical in a normal axis, so it is not chiral in 3D (the specular

image is coincident with the result of a rotation around a longitudinal axis), so there is no electromagnetic activity (no rotation). When taking into account the effect of the board, the structure becomes 3D chiral. In this case, we observe electromagnetic activity, which increases when the properties of the board (permittivity or losses) are higher, i.e., when there is more difference with free space.

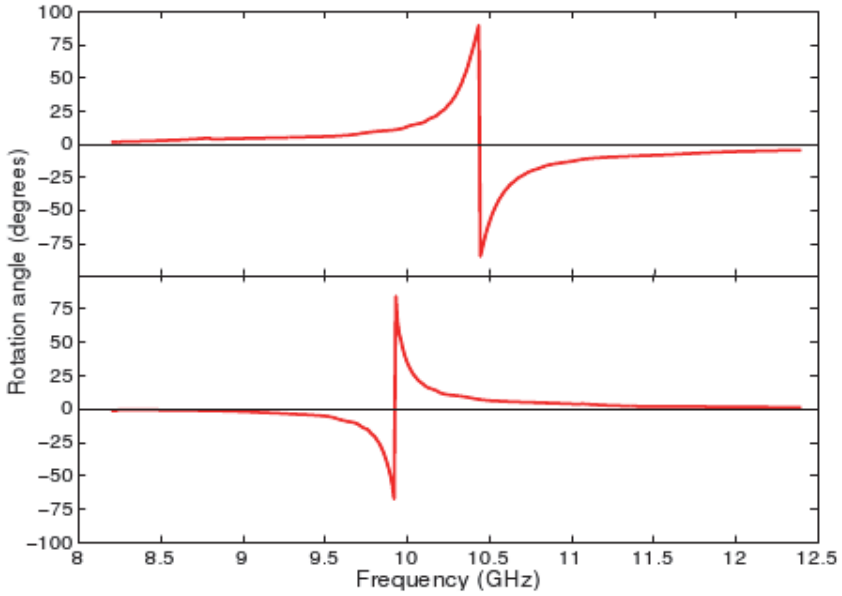

Fig. 12. Two examples of the rotation angle produced by a periodical lattice of metallic cranks formed by three equal size segments (5 mm) cranks for left-handed cranks with a separation of 6.9 mm (up) and right-handed cranks with a separation of 9.1 mm (down). [Reprinted from García-Collado et al. (2010) © 2010 IEEE]

4.3 Quasi-planar distributions (cranks)

Fig. 12 shows two examples of the rotation angle produced by periodical lattices of cranks as the one represented in Fig. 3. Both plots correspond to the cranks with the same total length, 15 mm, and different handedness and separation. It can be observed that the sign of the rotation produced by a periodical lattice of cranks depends on the handedness of the elements, as it has been observed in chiral composites formed by randomly oriented elements. In a periodical lattice, the distance of the elements also affects to the characteristic frequencies. In this case, the resonance frequency decreases from 10.4 GHz (up) to 9.8 GHz when the crank separation distance changes from 6.9 mm to 9.1 mm. We do not observe any non-reciprocal effect, i.e. the rotation angle is the same if the wave is incident in the opposite direction.

These results are compared with other ones, obtained by means of time-domain modeling of the same structure, using MeFisTo-3D. In this case, the four cranks of each gammadion are separated 6 mm, while there are 4 mm of distance between two consecutive gammadions. The results are showed in Fig. 13, showing a good agreement between both measures.

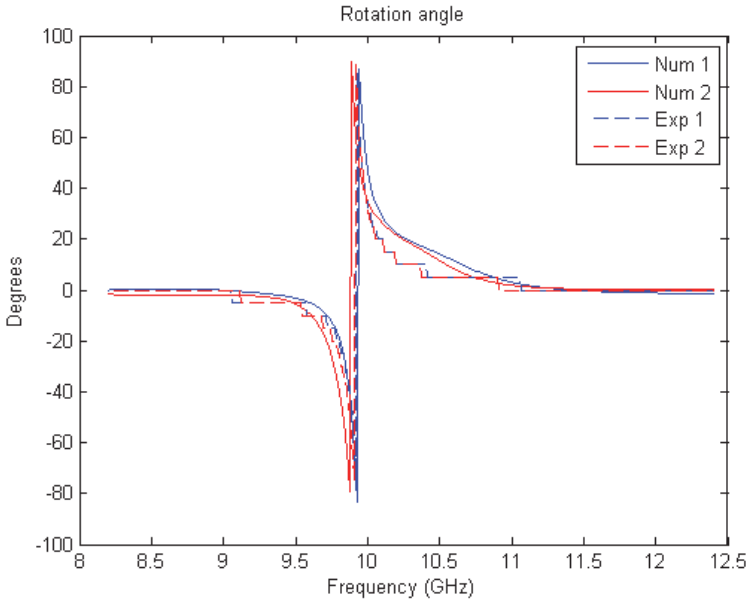

Fig. 13. Rotation of the polarization angle for a plane wave normally incident over a quasi-planar periodic array of right-handed cranks as shown in Figs. 3 and 6: numerical (Num) and experimental (Exp) results. 1 and 2 represent the two possible directions of the propagation wave (incident from front and back side, respectively).

Finally, we propose a different distribution of cranks (Fig. 14). In this case, there is a higher concentration of cranks in the same surface, so it is expected to obtain a higher gyrotropy too. That distribution is also geometrically reciprocal.

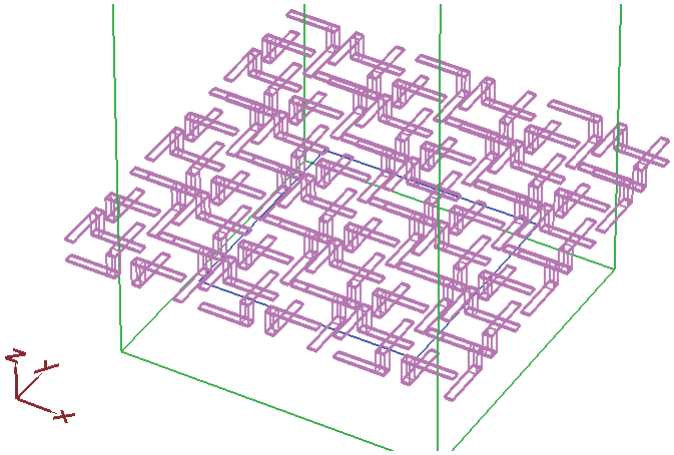

Fig. 14. MEFiSTo™ model of a condensed array of cranks. Each crank is composed by two arms, 3mm long, one in each side of the board (1.5 mm of thickness), plus a via connecting both.

The electromagnetic behavior of such distribution has been modeled using MEFiSTo™: we have obtained the rotation of the polarization plane after a normal transmission through that array. The angle of rotation does not depend on the initial polarization of the incident wave (that is, the medium behaves like a biisotropic one, at least in a transversal axis), and it is the same in the two directions of propagation (reciprocal). The result is shown in Fig. 15.
It is worth to mention the couple of discontinuities between -90º and 90º that may be observed in the figure. Such discontinuities are common to most of the distributions we have studied: when we see only one of them (Fig. 12 and Fig. 13) it is caused by the limitations in broadband that suffer our experimental bank. At the same time, other authors (Zhou et al., 2009) find a similar behavior in frequency, being usually assumed to correspond to resonance frequencies. We believe this behavior does not correspond to a real jump in the rotation frequency, but it is a consequence of the measurement procedure, in which the result is normalized between -90º and 90º. If we normalize between 0 y 180º the result in Fig. 15 would be as shown in Fig. 16.
More important: if we study the propagation through several layers of our material, we may draw the rotation angle like in Fig. 17. There, it is demonstrated that the response is lineal (the rotation angle is proportional to the width of the material (number of layers) and, then, the resonance frequency does not depend on the number of layers.

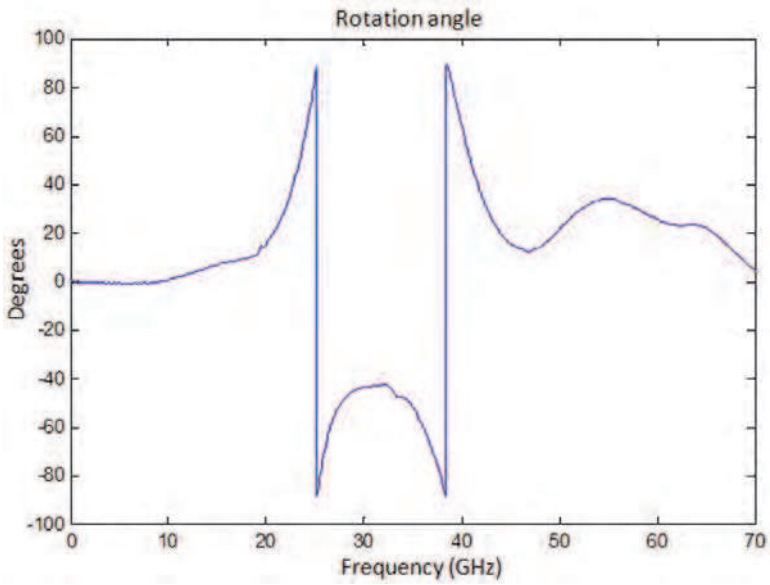

Fig. 15. Rotation of the polarization plane for a plane wave normally incident over a condensed array of cranks (Fig. 14), normalizing between -90º and 90º

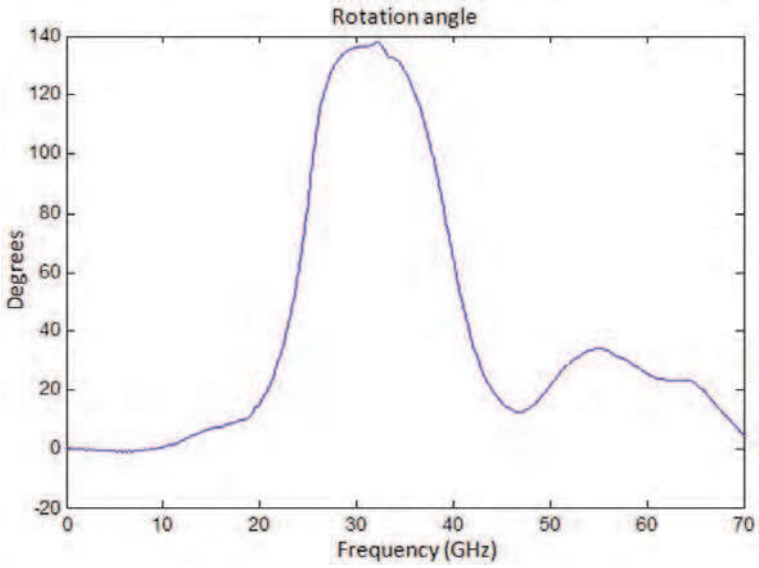

Fig. 16. Rotation of the polarization plane for a plane wave normally incident over a condensed array of cranks like represented in Fig. 14, normalizing between 0º and 180º

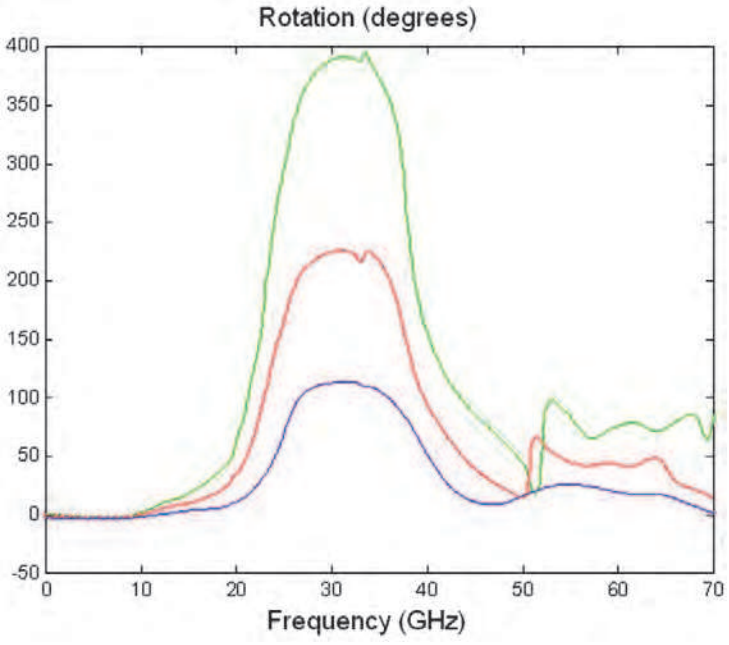

Fig. 17. Rotation of the polarization angle for a wave linearly polarized, incident over a condensed distribution of cranks like shown in Fig. 14, for one (blue line), two (red) or three (green) parallel boards. [Reprinted from Barba et al. (2009) © 2009 IEEE]

The chiral material for waveguide experiments was built as described in section 3. However, there are some inherent restrictions in the design due to the limited size of the sample. The radius of the waveguide is similar, in magnitude, to the one of the crank, which strongly limits the number of elements that can be placed on a one-layer distribution, without contact among the elements. Fig. 18 shows two examples produced by four metallic cranks in a foam host medium (left) and eight cranks (right). We have experimentally observed, as it could be deduced by considering symmetry reasons, that other distributions of cranks do not present an isotropic behavior.

In order to analyze the response of a single cell, we have measured the rotation angle after a transmission through a group of four cranks, making use of the waveguide setup described in section 3.Fig. 19 shows the rotation angle for cranks formed by equal-size segments, with a total length L ranging from 13.5 mm to 18 mm (Fig. 18). For example, for L = 15 mm, a clear resonance frequency is observed at f_0= 10.08 GHz, the angle is negative below f_0 and positive above f_0. It can be also observed that resonance frequency decreases when the length of the cranks increases, which is in agreement with similar observations found in composites formed by randomly oriented helices (Busse et al., 1999) or cranks (Molina-Cuberos et al., 2009). The experimental resonance frequencies are 8.24 GHz, 9.04 GHz, 10.1 GHz and 11.7 GHz, very close to a relation $\lambda = 2L$.

We have previously checked that the rotation angle does not depend on the relative orientation between cranks and incident wave, i.e. the sample presents an isotropic and homogeneous behavior. This fact does not occur in other configurations with odd number of cranks or with less symmetry properties. In the last case, the observed gyrotropy is a non-chiral effect and other electromagnetic effects, if any, hide the rotation due to chirality. In general we have found isotropic behavior when the sample presents symmetry under 45 degrees rotation, although other rotation symmetries are not ruled out.

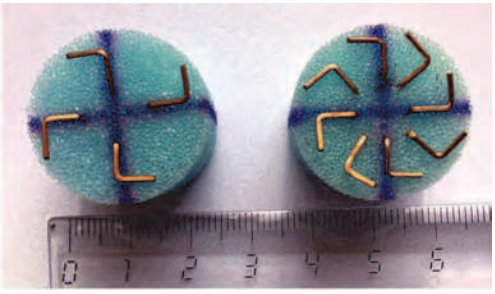

Fig. 18. Cylindrical samples used for the experimental determination of chiral effect by using a waveguide setup.

5. Conclusion

We have studied different periodical distributions, planar and quasi-planar, which show chiral behavior. We have observed that even when using a planar distribution, its electromagnetic activity comes from its 3D geometry. The rotation will be stronger, then, if we enhance this 3D characteristic. Two possibilities have been studied: some researchers prefer to use multilayered distributions of planar geometries, with a twist between adjacent layers, while we prefer to use two face metallization, with vias connecting both faces of

every board: that may present the advantage of obtaining similar electromagnetic activity, combined with thinner structures. The results we have obtained, both using numerical time-domain modeling and experimental measurements seem to support our claim

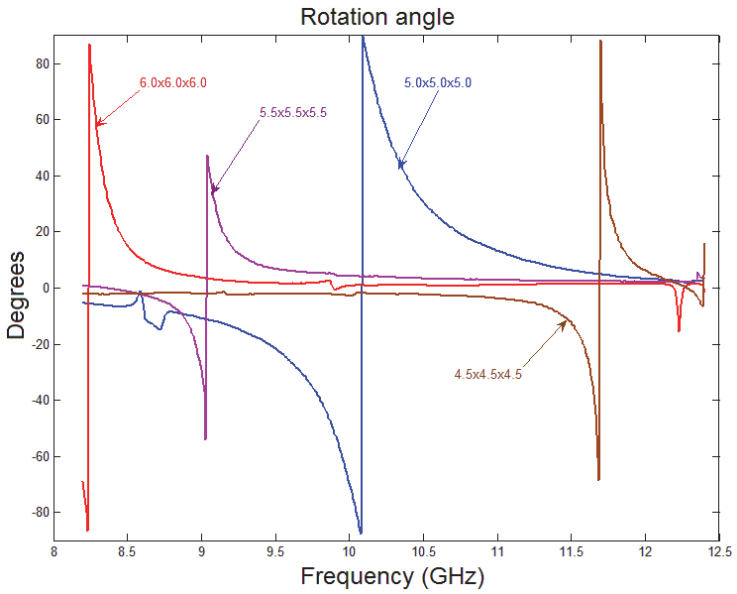

Fig. 19. Rotation angle produced by the samples composed by four cranks in foam (Fig. 18), as a function of the size of the cranks.

6. References

Alú, A.; Bilotti, F. & Vegni, L. (2003), Generalized transmission line equations for bianisotropic materials, *IEEE Transactions on Microwave Theory and Techniques*. Vol. 51, No. 11 (November 2003), pp. 3134–3141. ISSN 0018-9480.

Barba, I; Cabeceira, A.C.L.; Gómez, A. & Represa, J. (2009), Chiral Media Based on Printed Circuit Board Technology: A Numerical Time-Domain Approach, *IEEE Transactions on Magnetics*. Vol. 45, No. 3 (March 2009), pp. 1170-1173. ISSN 0018-9464.

Bahr, A.J. & Clausing, K.R. (1994). An approximate model for artificial chiral material, *IEEE Transactions on Antennas and Propagation*. Vol. 42, No. 12 (December 1994), pp. 1592-1599, ISSN 0018-926X.

Balanis, C.A. (1989). *Advanced Engineering Electromagnetics*, John Wiley & Sons, ISBN 0-471-62194-3, New York, NY, USA.

Brewitt-Taylor, C.R.; Lederer, P.G.; Smith F.C. & Haq S. (1999). Measurements and prediction of helix-loaded chiral composites, *IEEE Transactions on Antennas and Propagation*. Vol. 47, No. 4 (April 1999), pp. 692-700, ISSN 0018-926X.

Cloete, J.H.; Bingle, M. & Davidson, D.B. (2001). The Role of Chirality in Syntehtic Microwave Absorbers, *International Journal of Electronics and Communications*, Vol. 55, No. 4 (April 2001), pp. 233-239, ISSN 1434-8411.

Condon, E.U. (1937). Theories of optical rotatory power, *Reviews of Modern Physics,* Vol. 9, (October 1937), pp. 432-457, ISSN 0064-6861.

Demir, V.; Elsherbeni, A.Z. & Arvas, E (2005) FDTD formulation for dispersive chiral media using the Z transform method, *IEEE Transactions on Antennas and Propagation*, Vol. 53, No. 10 (October 2005), pp. 3374–3384, ISSN 0018-926X

García-Collado A.J.; Molina-Cuberos, G.J.; Margineda, J.; Núñez, M.J. & Martín, E. (2010). Isotropic and homogeneous behavior of chiral media based on periodical inclusions of cranks, *IEEE Microwaves and Wireless Components Letters,* Vol. 20, No 3, pp. 176-177, (March 2010), ISSN 1531-1309.

Gómez A.; Lakhtakia, A.; Margineda, J.; Molina-Cuberos, G.J; Núñez, M.J.; Saiz Ipiña, J.A, & Vegas A. (2008). Full-Wave hybrid technique for 3-D isotropic-chiral-material discontinuities in rectangular waveguides: Theory and Experiment, *IEEE Transactions on Microwave Theory and Techniques,* Vol. 56, No. 12 (December 2008), pp. 2815-2824, ISSN 0018-9480.

Gómez, A.; Lakhtakia, A.; Vegas, A. & Solano, M.A. (2010) Hybrid technique for analyzing metallic waveguides containing isotropic chiral materials, *IET Microwaves, Antennas & Propagation*, Vol. 4, No. 3 (March 2010), pp. 305-315, ISSN 1751-8725.

González-García, S.; Villó-Pérez, I.; Gómez-Martín, R. & García-Olmedo, B. (1998) Extension of Berenger's PML for bi-isotropic media, *IEEE Microwave and Guided Wave Letters*, Vol. 8, No. 9 (September 1998), pp. 297–299, ISSN 1051-8207

Kopyt, P.; Damian, R.; Celuch, M. & Ciobanu, R. (2010) Dielectric properties of chiral honeycombs – Modelling and experiment, *Composites Science and Technology*, Vol. 70, No. 7 (July 2010), pp. 1080-1088, ISSN 0266-3538.

Kuwata-Gonokami, M.; Saito, N.; Ino Y.; Kauranen, M.; Jefimovs, K.; Vallius, T.; Turunen, J. & Svirko, Y. (2005). Giant Optical Activity in Quasi-Two-Dimensional Planar Nanostructures, *Physical Review Letters*, Vol. 95, No. 22 (November 2005), pp. 227401, ISSN 0031-9007.

Lakhtakia, A.; Varadan, V.V. & Varadan, V.K. (1988) Radiation by a straight thin-wire antenna embedded in an isotropic chiral medium, *IEEE Transactions on Electromagnetic Compatibility*, Vol. 30, No. 1 (February 1988), pp. 84–87, ISSN 0018-9375.

Le Guennec, P. (2000a) Two-dimensional theory of chirality. I. Absolute chirality, *Journal of Mathematical Physics*, Vol. 41, No. 9 (September 2000), pp. 5954-5985, ISSN 0022-2488.

Le Guennec, P. (2000a) Two-dimensional theory of chirality. I. Relative chirality and the chirality of complex fields, *Journal of Mathematical Physics*, Vol. 41, No. 9 (September 2000), pp. 5986-6006, ISSN 0022-2488.

Lindell, I.V.; Tretyakov, S.A. & Oksanen, M.I. (1992) Conductor-backed Tellegen slab as twist polarizer, *Electronic Letters*, Vol. 28, No. 3 (30th January 1992), pp. 281–282, ISSN 0013-5194.

Lindell, I.V.; Sihvola, A.H.; Tretyakov, S.A. & Viitanen, A.J. (1994). *Electromagnetic Waves on Chiral and Bi-Isotropic Media*, Artech House, ISBN 0-89006-684-1, Norwood, MA, USA.

Lindman, K.F. (1920) Uber eine durch ein isotropes system von spiralformigen resonatoren erzeugte rotationspolarisation der elektromagnetischen wellen, *Annalen der Physik*, Vol. 368. No. 23 (May 1920), pp. 621–644, ISSN 1521-3889.

Marqués, R.; Jelinek, J. & Mesa, F. (2007). Negative refraction from balanced quasi-planar chiral inclusions, *Microwave and Optical technology Letters*, Vol. 49, No. 10 (October 2007), pp. 2606-2609, ISSN 0895-2477.

Molina-Cuberos, G.J.; García-Collado A.J.; Margineda, J.; Núñez, M.J. & Martín, E. (2009). Electromagnetic Activity of Chiral Media Based on Crank Inclusions, *IEEE Microwave and Wireless Components Letters*. Vol. 19, No. 5 (May 2009), pp. 278-280. ISSN 1531–1309.

Muñoz, J.; Rojo, M. Parreño, A. & Margineda J. (1998). Automatic measurement of permittivity and permeability at microwave frequencies using normal and oblique free-wave incidence with focused beam. *IEEE Transactions on Instrumentation and Measurement,* Vol 47, No. 4 (August 1998), pp. 886-892, ISSN 0018-9456.

Papakostas, A.; Potts, A.; Bagnall, D.M.; Prosvirnin, S.L.; Coles, H.J. & Zheludev, N.I. (2003). Optical Manifestations of Planar Chirality, *Physical Review Letters*, Vol. 90, No. 10 (March 2003), pp. 107404, ISSN 0031-9007.

Pendry, J.B. (2004). A Chiral Route to Negative Refraction, *Science*, Vol. 306, No. 5700 (November 2004), pp. 1353-1355, ISSN 0036-8075.

Pereda, J.A.; Grande, A.; González, O. & Vegas, A. (2006). FDTD Modeling of Chiral Media by Using the Mobius Transformation Technique, *IEEE Antennas and Wireless Propagation Techniques*, Vol. 5, No. 1 (December 2006), pp. 327–330, ISSN 1536-1225.

Pitarch, J.; Catalá-Civera, J.; Peñaranda-Foiz, F. & Solano, M.A. (2007). Efficient modal analysis of bianisotropic waveguides by the Coupled Mode Method, *IEEE Transactions on Microwave Theory and Techniques,* Vol. 55, No. 1 (January 2007), ISSN 0018-9480.

Plum, E.; Fedotov, V.A.; Schwanecke, A.S.; Zheludev, N.I. & Chen, Y. (2007). Giant optical gyrotropy due to electromagnetic coupling, *Applied Physics Letters*, Vol. 90, No. 22 (May 2007), pp. 223113, ISSN 0003-6951.

Plum, E.; Zhou, J.; Dong J.; Fedotov, V.A.; Koschny, T.; Soukoulis, C.M. & Zheludev, N.I. (2009). Metamaterial with negative index due to chirality, P*hysical Review B,* Vol. 79, No. 3 (January 2009), pp. 035407, ISSN 1098-0121.

Rogacheva, A. V.; Fedotov, V.A.; Schwanecke, A.S. & Zheludev, N.I. (2006). Giant Gyrotropy due to Electromagnetic-Field Coupling in a Bilayered Chiral Structure, *Physical Review Letters*, Vol. 97, No. 17 (October 2006), pp. 177401, ISSN 0031-9007.

Schwanecke, A.S.; Krasavin, A.; Bagnall, D.M.; Potts, A.; Zayats, A.V. & Zheludev, N.I. (2003). Broken Time Reversal of Light Interaction with Planar Chiral Nanostructures, *Physical Review Letters*, Vol. 91, No. 24 (December 2003), pp. 247404, ISSN 0031-9007.

Tretyakov, S.A.; Sihvola, A.H. & Jylhä, L. (2005). Backward-wave regime and negative refraction in chiral composites, *Photonics and Nanostructures: Fundamentals and Applications*, Vol. 3, No. 2-3 (December 2005), pp. 107–115, ISSN 1569-4410.

Varadan, V.K.; Varadan, V.V. & Lakhtakia, A. (1987). On the possibility of designing antireflection coatings using chiral composites, *Journal of Wave Matter Interaction*, Vol. 2 , No. 1 (January 1987), pp. 71–81, ISSN 0887-0586.

Viitanen, A.J. & Lindell, I.V. (1998). Chiral slab polarization transformer for aperture antennas, *IEEE Transactions on Antennas and Propagation*, Vol. 46 , No. 9 (September 1998), pp. 1395–1397, ISSN 0018-926X.

Xu, Y. & Bosisio, R.G. (21995) An efficient method for study of general bi-anisotropic waveguides, *IEEE Transactions on Microwave Theory and Techniques*, Vol. 43, No. 4 (April 1995), pp. 873–879, ISSN 0018-9480.

Zhou, J.; Dong, J.; Wang, W.; Koschny, T.; Kafesaki, M. & Soukoulis, C.M. (2009). Negative refractive index due to chirality, P*hysical Review B,* Vol. 79, No. 12 (March 2009), pp. 121104, ISSN 1098-0121.

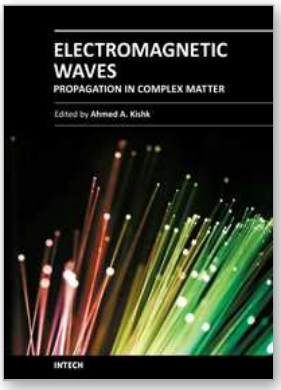

Electromagnetic Waves Propagation in Complex Matter
Edited by Prof. Ahmed Kishk

ISBN 978-953-307-445-0
Hard cover, 292 pages
Publisher InTech
Published online 24, June, 2011
Published in print edition June, 2011

This volume is based on the contributions of several authors in electromagnetic waves propagations. Several issues are considered. The contents of most of the chapters are highlighting non classic presentation of wave propagation and interaction with matters. This volume bridges the gap between physics and engineering in these issues. Each chapter keeps the author notation that the reader should be aware of as he reads from chapter to the other.

INTECH
open science | open minds

InTech Europe
University Campus STeP Ri
Slavka Krautzeka 83/A
51000 Rijeka, Croatia
Phone: +385 (51) 770 447
Fax: +385 (51) 686 166
www.intechopen.com

InTech China
Unit 405, Office Block, Hotel Equatorial Shanghai
No.65, Yan An Road (West), Shanghai, 200040, China
中国上海市延安西路65号上海国际贵都大饭店办公楼405单元
Phone: +86-21-62489820
Fax: +86-21-62489821